THE JOURNAL OF BIOLOGICAL CHEMISTRY
Vol. 276, No. 32, Issue of August 10, pp. 30188–30198, 2001

Printed in U.S.A.

Lipopolysaccharide Induces Rac1-dependent Reactive Oxygen Species Formation and Coordinates Tumor Necrosis Factor-α Secretion through IKK Regulation of NF-κB*

Received for publication, March 7, 2001, and in revised form, June 7, 2001
Published, JBC Papers in Press, June 11, 2001, DOI 10.1074/jbc.M102061200

Salih Sanlioglu‡§¶, Carl M. Williams‡§, Lobelia Samavati‡, Noah S. Butler‡, Guoshun Wang‖, Paul B. McCray, Jr.‖, Teresa C. Ritchie§, Gary W. Hunninghake‡, Ebrahim Zandi‡‡§§, and John F. Engelhardt‡§**¶¶**

*From the ‡Department of Internal Medicine-Division of Pulmonary and Critical Care, the §Center for Gene Therapy, **Department of Anatomy and Cell Biology, and ‖Department of Pediatrics, the University of Iowa College of Medicine, Iowa City, Iowa 52242, the ‡‡Department of Molecular Microbiology & Immunology, Norris Cancer Center, Los Angeles, California 90033, and the ¶Department of Medical Biology and Genetics, Akdeniz University, College of Medicine, Antalya, Turkey 07070*

Reactive oxygen species (ROS) are important second messengers generated in response to many types of environmental stress. In this setting, changes in intracellular ROS can activate signal transduction pathways that influence how cells react to their environment. In sepsis, a dynamic proinflammatory cellular response to bacterial toxins (*e.g.* lipopolysaccharide or LPS) leads to widespread organ damage and death. The present study demonstrates for the first time that the activation of Rac1 (a GTP-binding protein), and the subsequent production of ROS, constitutes a major pathway involved in NFκB-mediated tumor necrosis factor-α (TNFα) secretion following LPS challenge in macrophages. Expression of a dominant negative mutant of Rac1 (N17Rac1) reduced Rac1 activation, ROS formation, NFκB activation, and TNFα secretion following LPS stimulation. In contrast, expression of a dominant active form of Rac1 (V12Rac1) mimicked these effects in the absence of LPS stimulation. IKKα and IKKβ were both required downstream modulators of LPS-activated Rac1, since the expression of either of the IKK dominant mutants (IKKαKM or IKKβKA) drastically reduced NFκB-dependent TNFα secretion. Moreover, studies using CD14 blocking antibodies suggest that Rac1 induces TNFα secretion through a pathway independent of CD14. However, a maximum therapeutic inhibition of LPS-induced TNFα secretion occurred when both CD14 and Rac1 pathways were inhibited. Our results suggest that targeting both Rac1- and CD14-dependent pathways could be a useful therapeutic strategy for attenuating the proinflammatory cytokine response during the course of sepsis.

Septic shock induced by Gram-negative infections kills 50,000 to 100,000 people each year in the United States (1, 2). Sepsis is a systemic inflammatory response syndrome to a localized or systemic infection that leads to the overproduction of proinflammatory cytokines, such as TNFα,[1] and the ultimate failure of multiple organ systems. According to the Centers for Disease Control and Prevention, sepsis is the third leading cause of infectious death in the United States (3).

Lipopolysaccharide (LPS), an endotoxin found in the outer membrane of Gram-negative bacteria (4), is a major trigger of sepsis. Recognition of LPS is crucial for host antimicrobial defense reactions (5, 6). LPS stimulates mononuclear cells (monocytes and macrophages) and neutrophils to produce immunoregulatory and proinflammatory cytokines (interleukin-1, interleukin-6, TNF-α, TGF-β, and prostaglandins) (7–10). The myeloid differentiation antigen CD14, a 55-kDa glycosylphosphatidylinositol-anchored membrane glycoprotein (mCD14), has been shown to play essential roles in the activation of human mononuclear phagocytes by LPS (11–13). CD14 is expressed predominantly on the surface of monocytes, macrophages, and neutrophils, (11, 14–16) and it also exists as a soluble plasma protein lacking the glycosylphosphatidylinositol anchor (sCD14) (5, 17). Both forms have been shown to play crucial roles in the recognition of LPS and in the initiation of cellular immune responses by LPS (11, 14, 18). LPS-binding protein (LBP), a 60-kDa serum glycoprotein produced by the liver, has also been shown to enhance LPS-induced cytokine production by monocytic cells (19, 20). LBP binds to the lipid A region of LPS to form an LBP-LPS complex, which then interacts with CD14 to induce cytokine production (16, 21, 22). Identification of cell surface receptors (*e.g.* the Toll-like receptors (TLR)), which interact with the LPS-LBP-CD14 complex, has further elucidated the mechanisms of LPS induced signaling pathways (23).

Although CD14 and LBP are involved in LPS signaling (CD14-dependent pathways), the existence of additional signaling pathways (CD14-independent pathways) have been reported by other investigators (24–27). LPS antagonists, lipid Iva, and *Rhodobacter sphaeroides* lipid A, but not anti-CD14 blocking antibody, inhibited LPS-induced monocyte activation under

* This work was supported by National Institutes of Health NHLBI Grants HL60316 and DK54759 (to J. F. E.). A Leukemia and Lymphoma Special Fellow. The costs of publication of this article were defrayed in part by the payment of page charges. This article must therefore be hereby marked "*advertisement*" in accordance with 18 U.S.C. Section 1734 solely to indicate this fact.

§§ A Leukemia and Lymphoma Special Fellow.

¶¶ To whom correspondence should be addressed: Dept. of Anatomy and Cell Biology, University of Iowa, College of Medicine, 51 Newton Rd., Rm. 1-111 BSB, Iowa City, IA 52242. Tel.: 319-335-7744; Fax: 319-335-7198; E-mail: john-engelhardt@uiowa.edu.

[1] The abbreviations used are: TNFα, tumor necrosis factor-α; ROS, reactive oxygen species; LPS, lipopolysaccharide; LBP, lipopolysaccharide-binding protein; TLR, Toll-like receptor; GST, glutathione *S*-transferase; PAGE, polyacrylamide gel electrophoresis; FBS, fetal bovine serum; m.o.i., multiplicity of infection; PDTC, pyrrolidinedithiocarbamate; NAC, *N*-acetylcysteine; EMSA, electrophoretic mobility shift assay; PBS, phosphate-buffered saline; DMPO, 5,5-dimetyl-1-pyrroline *N*-oxide; DHE, dihydroethidium; RT-PCR, real time-polymerase chain reaction; HPRT, hypoxanthine-guanine-phosphoribosyl-transferase.

serum-free conditions (28). This suggested that these compounds act at a site distinct from CD14. In addition, neither LBP nor CD14 was found to be necessary for LPS-induced activation of bovine macrophages (29).

Human polymorphonuclear leukocytes are responsible for killing microorganisms and eliminating cellular debris. These functions are mediated by superoxide (O_2^-) generated by an NADPH-dependent oxidase, as well as other reactive oxygen species (ROS) such as hydrogen peroxide (H_2O_2), and hydroxyl radicals ($^{\cdot}OH$) (30). The assembly of NADPH oxidase has been shown to be up-regulated in neutrophils exposed to bacterial LPS (31). Furthermore, DeLeo *et al.* (31) have demonstrated that LPS priming increased the level of Rac2, a small GTP-binding protein associated with $p47^{phox}$ and $p67^{phox}$ (two subunits needed for NADPH oxidase function, $p91^{phox}$) at the membrane. These studies support a role for LPS priming of the respiratory burst in polymorphonuclear leukocytes. In addition, Rac1 (a homolog of Rac2) has been shown to control mitogenic and oncogenic signals through NADPH oxidase superoxide production (32, 33). However, little is known about a potential role of Rac1-NADPH oxidase complexes in controlling LPS-mediated intracellular signaling pathways. We hypothesized that Rac1 might be involved in LPS-mediated signaling pathways leading to the activation of macrophages. In the present study, we provide functional and biochemical evidence that Rac1 induction of NFκB is partially responsible for LPS-induced TNFα production. Activation of this pathway by LPS is dependent on Rac1-mediated ROS formation and the subsequent activation of the IKK complex, but appears to be independent of the CD14 receptor. These studies provide further definition of the ROS-mediated signal transduction pathways that contribute to LPS-induced TNFα secretion.

EXPERIMENTAL PROCEDURES

Preparation of Recombinant Adenoviruses—Eight recombinant adenoviral vectors expressing either β-galactosidase (Ad.CMVLacZ) (34), catalase (Ad.Cat) (35), a dominant negative mutant of Rac1 (Ad.N17Rac1) (36), a dominant active mutant of Rac1 (Ad.V12Rac1) (37), a dominant negative mutant form (K44M) of IKKα (Ad.IKKαKM), a dominant negative mutant form (K44A) of IKKβ (Ad.IKKβKA), a dominant negative mutant form (S32A/S36A) of IκBα (Ad.IkBM) (38), or a luciferase reporter gene driven by NFκB transcriptional activation (Ad.NFκBLuc), were used for functional studies. Ad.IKKαKM and Ad.IKKβKA were constructed from pRc-β actin plasmids encoding either the dominant negative mutant of IKKα (IKKαKM) or IKKβ (IKKβKA) (39). Fragments encoding the HA-tagged IKKαKM or IKKβKA cDNAs were excised by *Hin*dIII-*Not*I restriction digestion from pRc-β actin plasmids and blunt subcloned into the *Eco*RV site of the pAd.CMV-Link1 adenoviral shuttle plasmid. Recombinant adenoviruses were generated in 293 cells according to a procedure described by Anderson *et al.* (40). The expression of HA-IKKαKM or HA-IKKβKA from these replication defective adenoviral constructs was confirmed by Western blotting. pNFκB-Luc plasmid (CLONTECH Laboratories, Inc., Palo Alto, CA) was used to generate Ad.NFκBLuc vector. The fragment containing the luciferase gene driven by four tandem copies of the NFκB consensus sequence fused to a TATA-like promoter from the herpes simplex virus-thymidine kinase gene was released by *Kpn*I and *Xba*I double digestion. The *Kpn*I and *Xba*I fragment was inserted into a promoterless adenoviral shuttle plasmid (pAd5mcspA) (40) and Ad.NFκBLuc virus was generated by homologous recombination. Recombinant adenoviral stocks were generated as previously described (41) and were stored in 10 mM Tris with 20% glycerol at −80 °C. The particle titers of adenoviral stocks were determined by A_{260} readings and were typically 10^{13} DNA particles/ml. The functional titers of adenoviral stocks were determined by plaque titering on 293 cells and expression assays for encoded proteins. Typically the particle/plaque forming unit ratio was equal to 25.

Rac1 Activation Assay—Rac1 activation assays were performed using a modification of a previously described protocol (42). *pGEX-PBD* (PBD encodes the p21-binding domain of Pak1, an effector molecule that specifically binds activated Rac1) was kindly provided by Dr. Richard Cerione (43). GST-PBD fusion protein was purified from DL21 cells (Amersham Pharmacia Biotech, Piscataway, NJ) transformed with *pGEX-PBD*. Bacteria were grown at 37 °C to log phase and treated with 1 mM isopropyl-1-thio-β-D-galactopyranoside for 2 h. The cells were centrifuged and the cell pellet was resuspended in lysis buffer (20 mM Tris-HCl, pH 7.5, 100 mM NaCl, 5 mM $MgCl_2$, 0.5% Nonidet P-40, 1 mM phenylmethylsulfonyl fluoride, 10 μg/ml leupeptin, and 10 μg/ml aprotinin). Cells were then further lysed by 3 rounds of sonication (each lasting for 30 s). The lysate was subsequently centrifuged at 10,000 × *g* for 15 min, and the fusion protein was isolated from the supernatant using a Bulk GST Purification Kit (Amersham Pharmacia Biotech, Piscataway, NJ). The purified protein appeared as a single band on SDS-PAGE with Coomassie Blue staining. Protein concentrations were determined using the Bradford assay. For selective precipitation of GTP-bound Rac1, the GST-PBD fusion protein (50 μg) was prebound to agarose-conjugated anti-GST antibody (20 μg) (Santa Cruz Biotechnology, Inc., Santa Cruz, CA; catalog number sc-138 AC) in 500 μl of lysis buffer at 4 °C overnight. Subsequently, samples were centrifuged at 2500 × *g* for 5 min and then washed three times with lysis buffer. These PBD-bound agarose beads were used for precipitation of GTP-bound Rac1 from LPS-treated RAW cells as described below.

Confluent monolayers of RAW cells were treated with 0.2 μg/ml LPS (Sigma, catalog number L-2630, source *Escherichia coli* Sertotype 0111-B4, <1.3% protein, 3,000,000 endotoxin units/mg) and incubated at 37 °C for different periods of time (0, 5, 15, and 30 min). Cells were harvested into lysis buffer (20 mM Hepes, pH 7.4, 0.5% Nonidet P-40, 10 mM $MgCl_2$, 10 mM β-glycerophosphate, 10% glycerol, 10 μg/ml leupeptin, 10 μg/ml aprotinin) at the various time points by scraping. Precipitation of GTP-bound Rac1 was performed by the addition of 200 μg of RAW cell lysate to GST-PBD bound agarose beads for 2 h at 4 °C. Samples were then centrifuged at 2,500 × *g* for 5 min followed by three washes with lysis buffer. After boiling samples at 100 °C for 5 min in SDS-PAGE sample buffer followed by centrifugation, samples were loaded onto a 12% SDS-PAGE for Western blotting against anti-Rac1 antibodies. Nitrocellulose filters were blocked (5% non-fat dry milk in 1 × PBST) at 4 °C overnight followed by incubation with 0.2 μg/ml rabbit polyclonal anti-Rac-1 antibody (Santa Cruz Biotechnologies) diluted in blocking buffer for 1 h at 25 °C. Subsequently, the filter was washed and incubated with peroxidase-conjugated anti-rabbit IgG (Roche Molecular Biochemicals, Indianapolis, IN) at 0.9 μg/ml for 1 h at 25 °C. The filters were finally washed and developed using a chemiluminescence luminol reagent (Santa Cruz Biotechnologies, Santa Cruz, CA) and exposed to x-ray film. For loading controls, anti-GST antibody (B14) (Santa Cruz Biotechnology, catalog number sc-138) was used to probe the filters.

Tissue Culture and Infection—RAW 264.7 cells were obtained from ATCC and grown on 35-mm Petri dishes in Dulbecco's modified Eagle's medium with 10% FBS and 1% penicillin and streptomycin. Adenoviral infections were performed for 2 h at 37 °C, in Dulbecco's modified Eagle's medium without FBS. After infections, an equal volume of Dulbecco's modified Eagle's medium with 20% FBS was added to increase the serum concentration to 10% and the infections were continued for a total of 40 h. Most studies used various multiplicities of infection (m.o.i.) to test recombinant adenoviral vectors. In RAW cells, adenoviral infection at an m.o.i. of 5,000 particles/cell gave greater than >95% transduction as evidenced by transgene expression. A subset of RAW cells (<5%) appeared to be refractory to adenoviral infection even at m.o.i. of 10,000 particles/cell.

Luciferase Assay and TNFα Measurements—The luciferase assay system with Reporter Lysis Buffer (Promega, Inc., catalog number E4030) was used to measure NFκB-mediated transcriptional induction according to the manufacturer's protocol. All measurements of luciferase activity (relative light units) were normalized to the protein concentration. The NFκB responsive luciferase reporter, Ad.NFκBLuc, was used to co-infect cells at an m.o.i. of 5000 particles/cell in these experiments. For TNFα protein measurements, a DuoSet ELISA Development System Kit from R&D Systems (Minneapolis, MN, catalog number DY410) was used according to manufacturers instructions. Antioxidant chemicals pyrrolidinedithiocarbamate (PDTC, Sigma, catalog number P-8765) and *N*-acetylcysteine (NAC, Sigma, catalog number A-8199) were used to treat RAW cells for 1 h at 37 °C prior to LPS treatment at doses ranging from 1 to 100 μM (PDTC) and 1 to 25 μM (NAC).

Electrophoretic Mobility Shift Assays (EMSA)—Nuclear extracts were prepared according to the procedure published by Andrews and Faller (44). NFκB oligos (Promega, Madison, WI, catalog number E329B) were end-labeled using [γ-^{32}P]ATP and T4-kinase according to the manufacturers instructions. The mobility shift assays were performed as previously described (45).

Electron Spin Resonance Spectroscopy (ESR)—ESR was used to detect the production of hydroxyl radicals using a procedure modified from a previously published protocol (46). Briefly, ESR assays were conducted at room temperature using a Bruker model EMX ESR spectrometer (Bruker, Karlsvuhe, Germany) equipped with a TM_{110} cavity and a flat cell (Electron Spin Resonance Core Facility, University of Iowa, IA). Instrument settings were as follows: receiver gain, 1×10^6; modulation frequency, 100 kHz; microwave power, 40.1 mW; modulation amplitude, 1.0 G; sweep rate, 1.5 G/s. The WINEPR filter function, moving average ($n = 5$), was used to filter out noise in all spectra. Prior to LPS treatment, RAW cells were serum starved for 15 h, briefly trypsinized, and then resuspended in PBS with 0.5% FBS. The spin trap, 5,5-dimetyl-1-pyrroline *N*-oxide (DMPO), was added to cells at a final concentration of 50 mM. Cells then were immediately treated with LPS at a concentration of 5 μg/ml and the production of $^{\cdot}$OH was recorded for 45 min. Since the signal intensity decreased after 30 min, spectra recorded in the first 20 min were used for analysis. This procedure was also performed on RAW cells preinfected with Ad.N17Rac1, Ad.V12Rac1, or Ad.Cat virus at a m.o.i. of 10,000 particles/cell and incubated at 37 °C for 48 h prior to ESR analysis.

Dihydroethidium (DHE) Assays—DHE assays were performed according to a modified protocol from Miller and colleagues (47). Briefly, RAW cells were grown to 70% confluency on 6-well plates and serum starved overnight. The medium was then changed to PBS containing 10 μM DHE for 20 min at 37 °C prior to LPS stimulation. Cells were stimulated with LPS (5 μg/ml) in PBS containing 10 μM DHE and 0.5% FBS for 30 min at 37 °C. Cells were then scraped off the plates and kept on ice prior to fluorescence-activated cell sorter analysis. For experiments which included superoxide dismutase pretreatments, cells were incubated in PBS containing 1000 units/ml purified superoxide dismutase enzyme (Sigma, catalog number S2525) and 10 μM DHE for 20 min prior to LPS treatment. LPS (5 μg/ml) stimulation was carried out in PBS containing 10 μM DHE, 1000 units/ml superoxide dismutase, and 0.5% FBS for 30 min at 37 °C.

Real Time PCR—Total RNA was isolated using the Absolutely RNA RT-PCR Miniprep Kit according to manufacturers instructions (Stratagene, La Jolla, CA). RNA was quantified using the RiboGreen Kit (Molecular Probes, Eugene, OR). Total RNA was reversed transcribed to cDNA using the RETROscript RT-PCR Kit (Ambion, Austin, TX). PCR amplification was then performed in an iCycler iQ Fluorescence Thermocyler (Bio-Rad) as follows: 3 min at 95 °C, followed by 45 cycles of 20 s at 95 °C, 20 s at 58 °C, 20 s at 72 °C, and 10 s at 79 °C. Fluorescence data was captured during the dwell at 79 °C. Data were collected and recorded by iCycler iQ software (Bio-Rad) and expressed as a function of threshold cycle (C_t), the cycle at which the fluorescence intensity in a given reaction tube rises above background. Specific primer sets for murine *TLR* and *HPRT* genes were as follows (5′ → 3′): *TLR2* sense, TGGTTCTTTTCCCAAACTGG and antisense, GCTTTCTTGGGCTTCCTCTT; *TLR4* sense ATTGCTTGGCGAATGTTTCT and antisense, GACCCATGAAATTGGCACTC; *TLR6* sense TCTGCAACATGAGCCAAGAC and antisense, GTTTTGCAACCGATTGTGTG; *HPRT* sense, CCTCATGGACTGATTATGGAC and antisense, CAGATTCAACTTGCGCTCATC. Primers were selected based on nucleotide sequences downloaded from the National Center for Biotechnology Information data bank and designed with software by Steve Rozen and Helen J. Skaletsky ((1998) Primer3, code available at genome.wi.mit-.edu/genome_software/other/primer3.html). PCR conditions and data collection dwell temperature were based on melting curve analysis of each amplimer generated by the primers listed above. Data was captured at 4 °C below the lowest melting temperature among all amplimers assayed to ensure that primer-dimers were not contributing to the fluorescence signal generated with SYBR Green I DNA Dye. Relative quantitative gene expression was calculated as follows. For each sample assayed, the C_t for reactions amplifying *TLR2*, *TLR4*, *TLR6*, and *HPRT* were determined. *HPRT* was used as an internal reference. The C_t for each *TLR* gene was then corrected by subtracting the C_t for *HPRT* (ΔC_t). Untreated controls were chosen as the reference samples, and the ΔC_t for all LPS-treated experimental samples were subtracted from the ΔC_t for the control samples ($\Delta\Delta C_t$). Finally, LPS-treated *TLR2, TLR4,* and *TLR6* mRNA abundance relative to control *TLR2, TLR4*, and *TLR6* mRNA abundance was calculated by the formula $2^{-(\Delta\Delta Ct)}$. The validity of this approach was confirmed by using serial 10-fold dilutions of templates containing *TLR* and *HPRT* genes. Using this set of template mixtures, the amplification efficiencies for *TLR2, TLR4, TLR6*, and *HPRT* amplimers were found to be identical.

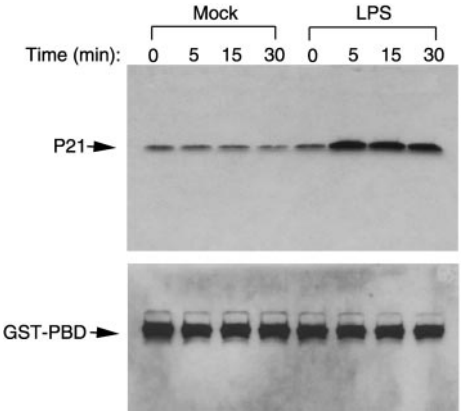

FIG. 1. **LPS activates Rac1.** Immunoprecipitation using a GST-PBD fusion protein that binds specifically to GTP-bound Rac1 (the active form) was used to detect the magnitude of Rac1 activation in response to LPS by Western blotting. RAW cells were treated with 0.2 μg/ml LPS or were mock treated for the exposure times (in minutes) indicated *above* each lane. 200 μg of RAW cell lysate from each condition was precipitated with GST-PBD and evaluated by Western blot against anti-Rac1 antibodies. The *top blot* indicates a representative anti-Rac1 Western with the p21 band (Rac1) indicated by an *arrow*. The same lysates were used in a Western blot against anti-GST antibodies as a loading control (*bottom blot*). The position of the GST-PBD protein is marked by an *arrow*.

RESULTS

LPS Activates the Rac1 Pathway—Previous reports have demonstrated that antioxidants significantly inhibit LPS-mediated activation of NFκB and subsequent TNFα secretion (48, 49). We hypothesized that Rac1 might be a central molecular regulator of LPS-induced changes in the cellular redox state promoting the induction of proinflammatory signal transduction pathways. In order to test whether Rac1 activity was elevated following LPS treatment, an assay developed by Glaven and colleagues (42) was utilized. This assay was used to specifically detect the abundance of GTP-bound (activated) Rac1 by immunoprecipitation with a GST-PBD fusion protein in a macrophage cell line (RAW). In support of our initial hypothesis, the abundance of GTP-bound Rac1 increased significantly as early as 5 min after treatment of RAW cells with LPS, but not in mock treated controls (Fig. 1). These studies indicate that Rac1 is activated early during the cellular response to LPS.

Rac1 Modulates LPS-induced NFκB Activity and TNFα Secretion—TNFα secretion following LPS challenge is well known to correlate with the induction of NFκB DNA binding activity (48, 50), which acts at sites in the TNFα promoter to induce expression. Given our results demonstrating the activation of Rac1 by LPS, we next sought to determine whether this pathway induces TNFα secretion via the NFκB signal transduction pathway. To approach this question, RAW cells were infected with a recombinant adenovirus expressing either the dominant negative mutant form of Rac1 (Ad.N17Rac1), or β-galactosidase (Ad.CMVLacZ) as a negative control, 48 h prior to LPS stimulation and assessment of TNFα levels in the media. As seen as in Fig. 2*A*, a maximal 41% reduction in TNFα secretion was achieved when RAW cells were infected with Ad.N17Rac1 at an m.o.i. 10,000 DNA particles/cell (the infection efficiency was >95%). This inhibitory response demonstrated a dose-dependent correlation with the particle dose of Ad.N17Rac1 virus used for infection. In contrast, no reduction in TNFα secretion was evident when cells were infected with the negative control virus Ad.CMVLacZ.

These results suggest that activation of Rac1 is required for a fraction, but not all, of the LPS-induced TNFα secretion. We next sought to investigate whether Rac1-dependent TNFα pro-

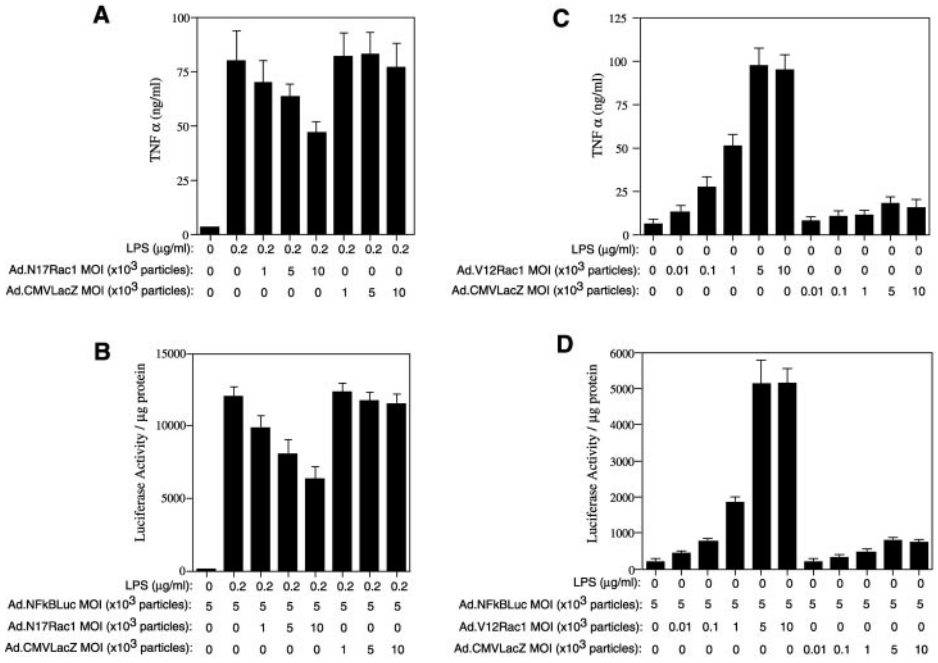

FIG. 2. **N17Rac1 expression downregulates LPS-induced NFκB transcriptional activity and TNFα secretion in RAW cells.** RAW cells were co-infected with Ad.NFκBLuc virus (m.o.i. of 5,000 particles/cell) together with Ad.N17Rac1 or Ad.CMVLacZ virus at increasing multiplicity of infections (particles/cell) as indicated *below* each graph. At 40 h post-infection, cells were stimulated with LPS (0.2 μg/ml) for 4 h at 37 °C. Cell supernatants were collected for enzyme-linked immunosorbent assay measurements of TNFα (*Panel A*) and cell lysates were subsequently harvested for NFκB-mediated luciferase activity assays (*Panel B*). Similar studies were performed by co-infecting cells with Ad.NFκBLuc virus (m.o.i. of 5,000 DNA particles/cell) together with increasing titers of Ad.V12Rac1 or Ad.CMVLacZ virus. In these experiments, cell supernatants and lysates were harvested at 35 h after infection in the absence of LPS stimulation. Results depict TNFα levels as determined by enzyme-linked immunosorbent assay (*Panel C*) and luciferase activity in relative light units (*Panel D*). Values in all graphs depict the mean (±S.E.) for four independent data points.

duction following LPS stimulation correlated with the activation of NFκB transcriptional activity. To initially test this hypothesis, RAW cells were co-infected with an adenovirus carrying an NFκB responsive luciferase reporter gene (Ad.NFκBLuc) in combination with Ad.N17Rac1 or Ad.CMVLacZ. Luciferase assays were then performed to assess NFκB transcriptional activity. As seen in Fig. 2*B*, reductions in NFκB reporter activity in the presence of N17Rac1 expression closely mirrored reductions seen in TNFα production (Fig. 2*A*). Maximal inhibition of NFκB transcriptional activity reached 47% when RAW cells were infected with the Ad.N17Rac1 virus at an m.o.i of 10,000 DNA particles/cell. No such reduction was evident when RAW cells were infected with he Ad.CMVLacZ virus. These results were confirmed by analysis of NFκB DNA binding activity using EMSA. In these studies RAW cells were infected with either Ad.N17Rac1 or Ad.CMVLacZ for 48 h prior to LPS treatment and the preparation of nuclear extracts. As seen in Fig. 3*A*, Ad.N17Rac1, but not Ad.CMVLacZ, reduced NFκB heterodimer complex formation (p50/p65) induced by LPS. The reduction in NFκB DNA binding invoked by the expression of N17Rac1 was ~50% and closely paralleled findings from the luciferase reporter assays (Fig. 2*B*). These results indicate that a significant fraction of LPS-induced TNFα secretion is mediated via Rac1 activation of NFκB.

Constitutive Activation of Rac1 Mimics LPS Induction of NFκB Activity and TNFα Secretion—As an alternative approach for demonstrating a causal link between NFκB induction by Rac1 and TNFα secretion, we tested whether expression of a dominant, constitutively active, form of Rac1 (V12Rac1) could mimic the effects of LPS treatment and lead to the induction of both NFκB and TNFα secretion. As seen in Fig. 2*C*, a 16-fold maximal induction in TNFα secretion was obtained when RAW cells were infected with Ad.V12Rac1 virus at an m.o.i. 5000 DNA particles/cell. Importantly, this induction in TNFα secretion was achieved in the absence of LPS stimulation and also demonstrated a clear dose response with the amount of virus used for infection. In contrast, only a slight induction of TNFα secretion was detected with Ad.CMVLacZ virus at similar multiplicity of infections. The induction of TNFα by V12Rac1 also clearly correlated with the activation of NFκB transcriptional activity, as indicated by a 25-fold increase in luciferase reporter expression following co-infection with Ad.NFκBLuc and Ad.V12Rac1, each at an m.o.i. of 5000 DNA particles/cell (Fig. 2*D*). EMSA analysis of cells expressing V12Rac1 demonstrated a direct correlation in the level of induced NFκB DNA binding and TNFα expression (Fig. 3*B*). Furthermore, both TNFα secretion and NFκB DNA binding induced by expression of the constitutively active V12Rac1 mutant was nearly completely blocked by co-expression of an IkBα mutant that blocks NFκB activation (IκBα S32A/S36A), but not by LacZ (Fig. 3, *B* and *C*). Taken together, these studies substantiate the hypothesis that Rac1 primarily induces TNFα production through the NFκB pathway. Since these studies with V12Rac1 were performed in the absence of LPS stimulation, the results indicate that Rac1 activation is a major effector of the proinflammatory signaling cascade distal to LPS receptor activation.

LPS Activation of Rac1 and Constitutively Active V12Rac1 Mediate NFκB-dependent TNFα Secretion through Activation of Both IKKα and IKKβ—Two adenoviral constructs expressing either the dominant mutant of IKKα (Ad.IKKαKM) or IKKβ (Ad.IKKβKA) were generated to elucidate mechanisms by which Rac1 activates NFκB-dependent TNFα secretion. As shown in Fig. 4*A*, both recombinant constructs produced HA-tagged IKK subunits as detected by Western blot following infection in HeLa cells. We next sought to determine whether both IKKα and IKKβ were required for Rac1 mediated activation of NFκB and subsequent TNFα expression. Two experimental conditions were evaluated, LPS induction of Rac1 and constitutive activation of Rac1 (using infection with Ad.V12Rac1) in the absence of LPS. As shown in Fig. 4, both LPS treatment and expression of V12Rac1 stimulated TNFα secretion (Fig. 4*B*) and NFκB-dependent transcription (Fig. 4*C*). LPS-induced TNFα secretion was most significantly inhibited following infection at the highest multiplicity of infections with Ad.IKKβKA (6.1-fold) as compared Ad.LacZ infected controls. Ad.IKKαKM infection at an identical multiplicity of infection led to a 1.7-fold blunting of LPS-induced TNFα secretion. Similarly, V12Rac1-induced TNFα secretion was more significantly blocked by IKKβKA (5.1-fold) as compared with Ad.IKKαKM (2.5-fold). Interestingly, IKKβKA preferentially inhibited NFκB-dependent transcription following LPS stimulation (30-fold) or expression of V12Rac1 (18.2-fold) as compared with IKKαKM (2.5–2.9-fold) (Fig. 4*D*). These finding

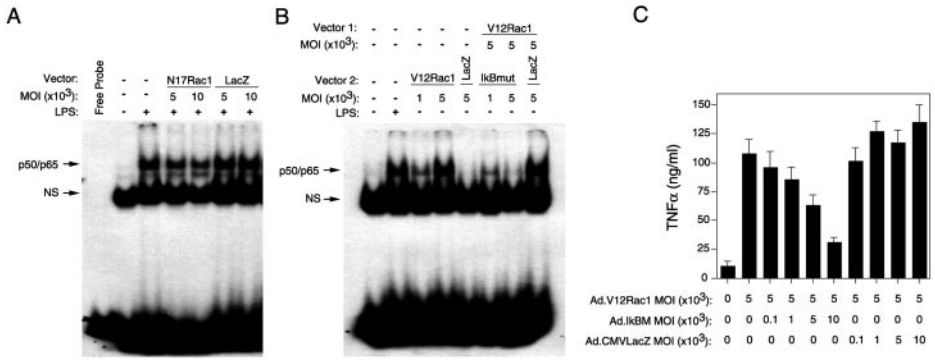

FIG. 3. **NFκB activation occurs via the Rac1 pathway leading to the induction of TNFα expression.** In order to confirm that Rac1 regulates NFκB transcriptional activation following LPS stimulation, EMSA was used to evaluate the level of NFκB DNA binding in nuclear extracts from RAW cells infected with Ad.N17Rac1 (*Panel A*) or Ad.V12Rac1 (*Panel B*) viruses. *Panel A* depicts experiments performed in RAW cells infected with either Ad.N17Rac1 or Ad.CMVLacZ virus at increasing multiplicity of infections for 40 h prior to stimulation with LPS (0.2 μg/ml). Nuclear extracts were prepared at 2 h post-LPS treatment and the experimental conditions for each lane are indicated *above* the gel. The p50/p65 heterodimer of NFκB and nonspecific shifted bands (*NS*) are indicated by *arrows* to the *left* of the gel. *Panel B* depicts EMSA results evaluating NFκB DNA binding in RAW cells infected with Ad.V12Rac1, Ad.CMVLacZ, and/or Ad.IkBM. In these experiments, cells were preinfected with Ad.CMVLacZ or Ad.IκBM for 30 h prior to superinfection with Ad.V12Rac1 for an additional 30 h. Nuclear extracts were prepared at 30 h (single vector conditions) and 60 h (dual vector conditions) following the initial infection in the absence of LPS stimulation. As a control, nuclear extracts were also prepared at 2 h after LPS treatment in uninfected cells. The experimental conditions for each lane are indicated *above* the gel. Results in *Panels A* and *B* are representative of three independent experiments performed in duplicate. *Panel C* depicts enzyme-linked immunosorbent assay results quantifying TNFα secretion under conditions similar to those in *Panel B*. All experimental conditions in *Panel C* were performed in the absence of LPS stimulation. RAW cells were infected with either the Ad.IkBM or Ad.CMVLacZ virus at increasing multiplicity of infection at 37 °C for 30 h. Later, these cells were also infected with Ad.V12Rac1 virus at an m.o.i. of 5000 DNA particles/cell for an additional 35 h prior to harvesting supernatants for TNFα secretion. Viral vectors used for infection and the multiplicity of infection (particles/cell) used are given *below* the graph. Values represent the mean (±S.E.) of four independent data points.

suggest that IKKβ may play a more dominant role than IKKα in NFκB transcriptional activation following LPS induction of Rac1. However, the ~50% reduction in NFκB transcriptional activity by IKKαKM is somewhat different than previous reports suggesting little or no contribution of IKKα to IKK activity following proinflammatory stimuli (51, 52). This difference may be attributable to the higher level of transgene expression achieved in the current study with recombinant adenoviral vectors.

LPS Stimulation of RAW Cells Leads to the Generation of Superoxide Radicals—The assembly of NADPH oxidase has been previously shown to be activated in neutrophils by exposure to bacterial LPS (31). In neutrophils, this NADPH oxidase complex is responsible for the generation of superoxide, an important component of antibacterial activity in respiratory burst. Unlike neutrophil NADPH oxidase gp91, which as a transmembrane protein generates superoxides topologically in the extracellular compartment, other families of NADPH oxidases that generate intracellular superoxide proposed to act as second messengers important to intracellular signaling pathways have been recently identified (53–55). In order to test whether LPS treatment leads to the generation of ROS, ESR was performed using the spin trap, DMPO (46). As seen in Fig. 5*C*, treatment of RAW cells with LPS gave rise to significant levels of DMPO/˙OH spin adduct. Generation of LPS-induced DMPO/˙OH was significantly attenuated by infection with the dominant negative Ad.N17Rac1 (Fig. 5*D*). In contrast, expression of the constitutively active V12Rac1 mutant gave rise to extremely high levels of DMPO/˙OH even in the absence of LPS stimulation (Fig. 5*E*). This was not seen when the N17Rac1 negative mutant form of the protein was expressed in the absence of LPS (Fig. 5*B*).

Although these data are consistent with the generation of hydroxyl radicals following LPS stimulation, they presently cannot discriminate between superoxides as the precursor ROS responsible for DMPO adducts seen in our studies. DMPO can also react with superoxide (O_2^-) to form the DMPO/˙OOH superoxide adduct of DMPO. DMPO/˙OOH can then be rapidly converted to the DMPO/˙OH spin adduct. This spin adduct is indistinguishable from the DMPO/˙OH formed by direct trapping of authentic ·OH (56, 57). Therefore, it was necessary to determine if the DMPO/˙OH adduct was generated by initial trapping of O_2^- or from the trapping of authentic ˙OH (58). Infection with the Ad.N17Rac1 virus dramatically decreased the magnitude of LPS-induced DMPO/˙OH spectra as shown in Fig. 5*D*. It is common knowledge that Rac1 activates NADPH oxidase to produce O_2^- (32). Since N17Rac1 expression inhibited LPS-induced DMPO/˙OH radical formation in our assays, it is most likely that O_2^- is the precursor to the DMPO/˙OH adduct recorded during ESR analysis. It is also possible that ˙OH radicals might be generated from H_2O_2 via a Fenton reaction. In order to test this hypothesis, RAW cells were infected with an adenovirus encoding catalase enzyme (Ad.Cat) (35). Infection with the Ad.Cat virus (Fig. 6, *D* and *E*) partially quenched the LPS-induced DMPO/˙OH adduct (Fig. 6, *B* and *C*). These findings suggest that a significant portion of the LPS-induced DMPO/˙OH adduct must be derived from H_2O_2, most likely via a Fenton reaction.

The most likely origin of H_2O_2 following LPS stimulation would be expected to come from NADPH oxidase derived O_2^- following dismutation by intracellular superoxide dismutase. However, since ESR is incapable of directly distinguishing between ˙OH and O_2^- radical formation, additional assays were designed to confirm the generation O_2^-. The DHE assay (47), which is fairly specific for O_2^- (59), was used to test whether the source of LPS-induced ROS was O_2^-. These DHE assays clearly demonstrated a significant increase in DHE fluorescence following treatment of RAW cells with LPS and suggested that O_2^- radicals are, at least in part, a precursor ROS formed following LPS stimulation (Fig. 7). Furthermore, pretreatment of RAW cells with purified superoxide dismutase enzyme quenched the majority of LPS-induced O_2^- production (Fig. 7). Both the DHE assay (with superoxide dismutase treatment) and the ESR results (with Ad.N17Rac1 infection) clearly suggest that O_2^- is a major induced form of ROS in RAW cells following LPS stimulation.

Reactive Oxygen Species Are Critical for LPS-induced TNFα Secretion—We have clearly demonstrated that LPS treatment

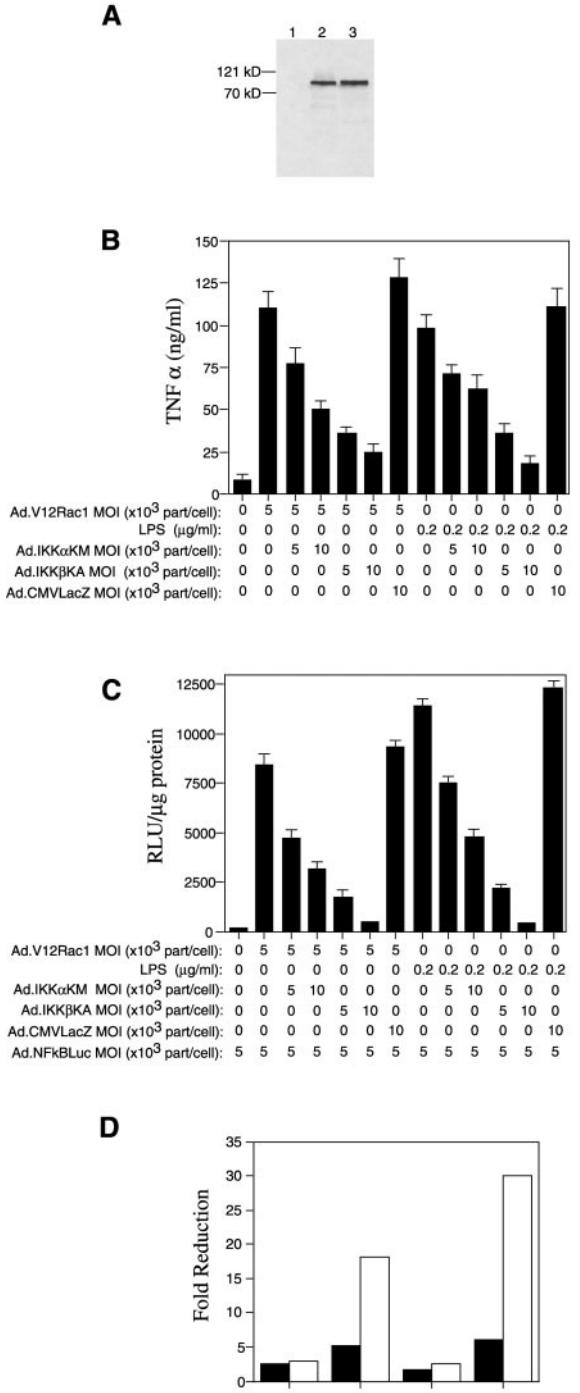

FIG. 4. **IKKβ is preferentially required for Rac1 induction of NFκB following LPS stimulation.** Two recombinant adenoviral vectors, Ad.IKKαKM and Ad.IKKβKA, were used to probe the functional involvement of the IKK complex in LPS/Rac1-mediated activation of NFκB and TNFα expression. *Panel A* depicts a Western blot of cellular lysates from HeLa cells infected with either Ad.IKKαKM or Ad.IKKβKA (m.o.i. of 5000 particles/cell). Blots were probed with anti-HA peroxidase antibody (Roche Molecular Biochemicals) and developed using ECL. *Lane 1*, control uninfected; *lane 2*, IKKαKM infected; *lane 3*, IKKβKA-infected cell lysates. Molecular standard markers (β-galactosidase (121 kDa) and bovine serum albumin (70 kDa)) are indicated to the *left* of the blot. In *Panels B-D*, RAW cells were infected with Ad.IKKαKM, Ad.IKKβKA, or Ad.LacZ 30 h prior to infection with Ad.V12Rac1 virus at the indicated multiplicity of infections. Supernatants were harvested 35 h after Ad.V12Rac1 infection for analysis of TNFα levels by enzyme-linked immunosorbent assay (*Panel B*). As a comparison to Ad.V12Rac1-infected cells, RAW cells were infected with Ad.IKKαKM, Ad.IKKβKA, or Ad.LacZ 48 h prior to treatment with LPS for 4 h after which supernatants were harvested for analysis of TNFα levels by enzyme-linked immunosorbent assay (*Panel B*). NFκB transcriptional activity using Ad.NFκBLuc-infected cells was similarly evaluated in *Panel C*. In these experiments RAW cells were infected with Ad.NFκBLuc virus 35 h prior to harvesting. Viral vectors used for infection and the multiplicity of infection (particles/cell) used are given *below* the graph. The timing of viral infections was identical to that shown in *Panel B*. Values represent the mean (±S.E.) for three independent data points. *Panel D* depicts the fold-reduction in TNFα expression (*solid bars*) and NFκB-mediated luciferase activity (*open bars*) in the presence of Ad.IKKαKM or Ad.IKKβKA. Fold reductions were calculated from the mean values in the presence of each of these dominant mutants as compared with infection with Ad.LacZ.

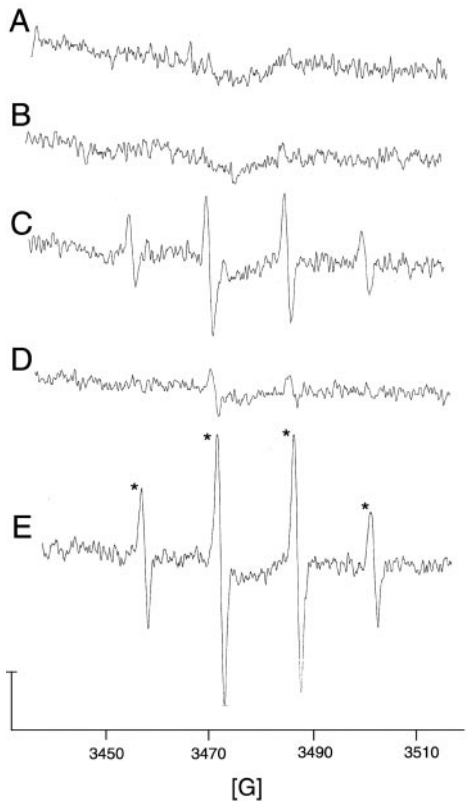

FIG. 5. **Rac1 mediates ROS formation in RAW cells following LPS stimulation.** RAW cells were trypsinized and resuspended (2×10^6 cells/ml) in phosphate-buffered saline with 0.5% FBS. DMPO was added to cells just prior to measurements. When applicable, LPS (5 μg/ml) was added immediately after DMPO. When indicated, cells were infected (10,000 particles/cell) with recombinant adenoviruses at 40 h prior to trypsinization for ESR assays. ESR measurements were recorded for 20 min after the addition of DMPO. The spectra are from cells treated under the following conditions: *A,* uninfected cells with no LPS treatment; *B,* Ad.N17Rac1-infected cells without LPS treatment; *C*, LPS-treated cells without infection; *D,* Ad.N17Rac1-infected cells treated with LPS; *E,* Ad.V12Rac1-infected cells without LPS treatment. *Asterisks* in *Panel E* mark the DMPO-hydroxyl radical adduct. The *bar* on the *y* axis represents 5×10^4 arbitrary units of intensity and the same scale is used for all panels. The *x* axis represents magnetic field in Gauss. $a^N = a^H = 14.9$ G is the hyperfine splitting constant for the DMPO/˙OH adduct. Spectra shown are representative of at least two independent experiments.

of RAW cells induces the production of ROS as determined by ESR. Although Ad.N17Rac1 expression reduced the production of ROS radicals in response to LPS treatment, the absolute requirement for ROS in the activation of NFκB and subsequent TNFα production remains unclear. Two potential hypotheses could explain the current findings. First, ROS generated by activated Rac1 could be an unrelated effect of activating this pathway and may not be required for NFκB activation or TNFα expression. Alternatively, Rac1-activated ROS production

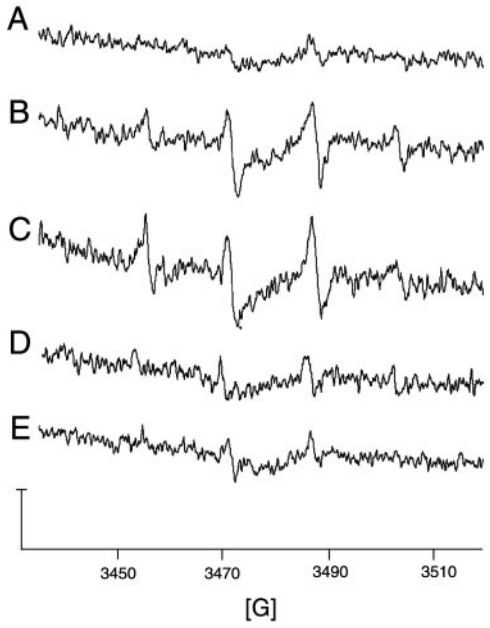

FIG. 6. **Catalase expression blocks induction of the DMPO/˙OH adduct following LPS treatment.** RAW cells were either uninfected or infected with Ad.Cat vector at an m.o.i. of 10,000 DNA particles/cell for 48 h prior to LPS treatment. ESR recordings were carried out as described under "Experimental Procedures." *Panel A* shows untreated cells. *Panels B* and *C* show two independent sets of cells treated with LPS (5 μg/ml) in the absence of infection. *Panels D* and *E* are two independent sets of cells infected with Ad.Cat and treated with LPS (5 μg/ml). The *y* axis represents 5×10^4 arbitrary units of intensity and the same scale was used for all conditions. The *x* axis is the magnetic field in Gauss.

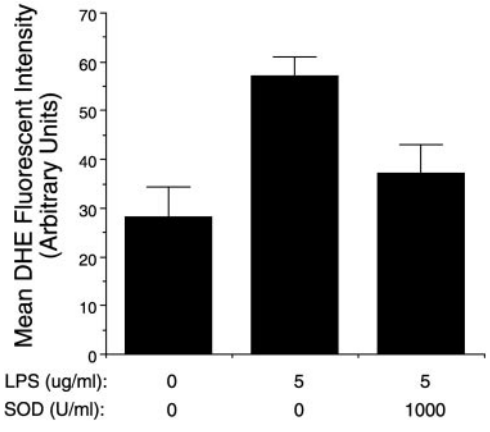

FIG. 7. **LPS generates superoxide radicals in RAW cells.** DHE assays were employed to evaluate superoxide radical formation following LPS exposure as described under "Experimental Procedures." Cells were pretreated with DHE (with and without superoxide dismutase (*SOD*) enzyme) followed by exposure to LPS. The mean fluorescent intensity (as determined by fluorescence-activated cell sorter analysis) is given on the *y* axis. Various treatment conditions are provided on the *x* axis. The data represents the mean (±S.E.) of six independent data points from two independent experiments.

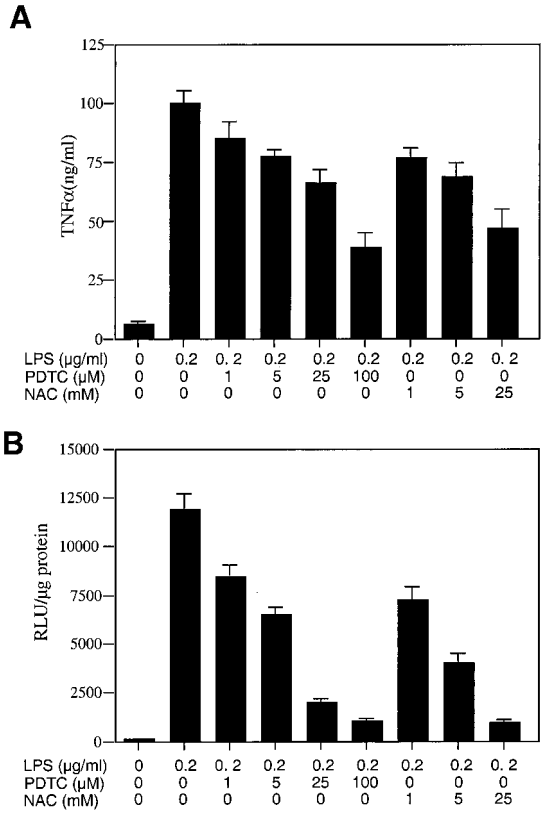

FIG. 8. **ROS are important mediators of LPS-induced TNFα secretion.** RAW cells were infected with Ad.NFκBLuc (5,000 particles/cell) for 40 h prior to treatment with the indicated amounts (below each graph) of PDTC or NAC for 1 h at 37 °C. Subsequently, cells were stimulated with LPS (0.2 μg/ml) in the continued presence of antioxidants in the culture media and supernatants were harvested 4 h later for TNFα assay. The concentration of TNFα was determined by the enzyme-linked immunosorbent assay (*Panel A*) and the level of NFκB transcriptional activation was assessed by luciferase activity (*Panel B*). Values represent the mean (±S.E.) of four independent data points.

could be integral to the activation of NFκB and TNFα expression. In order to differentiate between these two potential mechanisms, we performed studies evaluating LPS-induced NFκB transcriptional activation and TNFα production under conditions where intracellular ROS were quenched by the use of chemical scavengers. These studies utilized two chemical scavengers, PDTC and NAC, which have been shown to quench superoxides (60), hydrogen peroxide (61, 62), and hydroxyl radicals (60, 62). RAW cells were treated with increasing concentrations of either PDTC or NAC for 1 h at 37 °C prior to LPS treatment. As seen in Fig. 8*A*, 34 and 61% reductions of TNFα expression were obtained when RAW cells were treated with 25 or 100 μM PDTC, respectively. Similarly, treatment of RAW cells with 25 mM NAC reduced TNFα production by 54%. In order to assess the effect of these antioxidants on NFκB transcriptional activity, studies were performed using RAW cells preinfected with the luciferase reporter virus Ad.NFκBLuc (m.o.i. of 5000 DNA particles/cell) prior to treatment with antioxidants (PDTC or NAC) and LPS treatment (Fig. 8*B*). These results demonstrated that LPS-induced NFκB-mediated luciferase activity was reduced in a dose-dependent fashion when RAW cells were treated with these antioxidants. Interestingly, the antioxidant invoked reduction in NFκB transcriptional activation was much more complete than their effect on TNFα secretion. Together with earlier findings, these results support the hypothesis that Rac1-mediated ROS production may primarily act to induce NFκB activation following LPS stimulation. However, it is also clear that activation of the Rac1 signaling cascade and subsequent ROS production accounts for only a portion of the LPS-mediated cellular responses leading to expression of TNFα.

CD14 Blocking Antibodies Decrease LPS-induced TNFα Secretion Independent of Rac1—Our results thus far demonstrate that Rac1 plays a critical role in ROS-mediated activation of NFκB and subsequent TNFα secretion. However, since N17Rac1 blocked only about half of the LPS-induced TNFα production, our results also suggest that alternative pathways likely contribute to the activation of TNFα. This is consistent

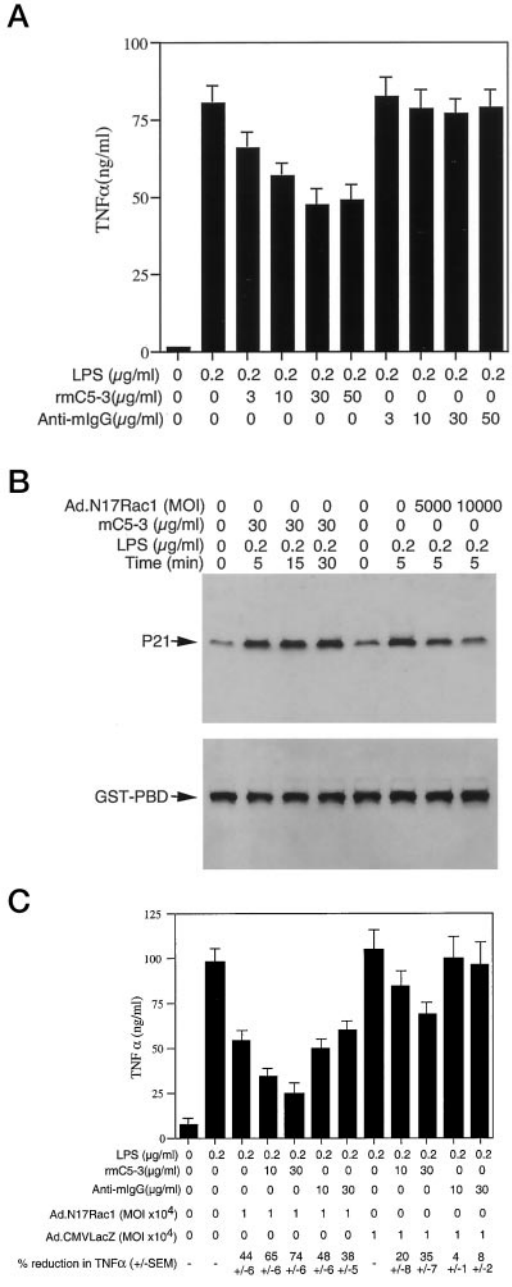

FIG. 9. **LPS activation of Rac1 is independent of CD14 receptor activation.** CD14 blocking antibodies were used to evaluate the extent of CD14 receptor activation needed for LPS-induced TNFα secretion (*Panel A*). RAW cells were treated with increasing concentrations of either anti-CD14 blocking antibody (rmC5-3) or anti-mouse IgG for 1 h at 37 °C. Then cells were stimulated with LPS (0.2 μg/ml) in the continued presence of antibodies for 4 h at 37 °C. Supernatants were collected for evaluation of TNFα levels as determined by enzyme-linked immunosorbent assay. Values represent the mean (±S.E.) of four independent data points for each condition. The involvement of the CD14 receptor in Rac1 activation was similarly evaluated in *Panel B*. RAW cells were either pretreated with anti-CD14 receptor antibody for 1 h at 37 °C or infected with Ad.N17Rac1 (10,000 particles/cell) for 40 h prior to LPS (0.2 μg/ml) stimulation. The abundance of GTP-bound Rac1 was then evaluated at 5 to 30 min post-LPS treatment by immunoprecipitation with GST-PBD followed by Western blotting with anti-Rac1 antibody (*upper panel*). Duplicate Western blots were also probed with anti-GST antibody as a control for loading (*lower panel*). The combined ability of both anti-CD14 antibody and N17Rac1 to inhibit TNFα secretion following LPS treatment was evaluated in *Panel C*. RAW cells were infected with either the Ad.N17Rac1 or Ad.CMVLacZ virus at m.o.i. of 10,000 particles/cell for 40 h prior to treatment with either rmC5-3 or anti-mIgG antibodies at the indicated concentrations for 1 h. Cells were then treated with LPS (0.2 μg/ml) for 4 h in the continued presence of rmC5-3 or anti-mIgG antibodies. Supernatants were harvested for enzyme-linked immunosorbent assay determination of TNFα. Conditions for each experimental point are indicated *below* the graph with the percent reduction in TNFα secretion. Values represent the mean (±S.E.) of three independent data points for each condition.

with previous reports of both CD14-dependent (16, 21, 22) and CD14-independent (24–27) pathways in the mediation of LPS-induced TNFα expression. Therefore, it seemed essential to investigate a possible association of Rac1 with CD14. In an initial effort to address this question, CD14-dependent pathways were blocked using CD14 blocking antibodies and the effects on Rac1 activation and TNFα production were evaluated. The blocking antibody used, RmC5-3, has previously been demonstrated to block LPS-induced CD14-mediated signaling pathways (63, 64). As seen in Fig. 9*A*, treatment of RAW cells with RmC5-3 CD14 blocking antibodies prior to LPS stimulation significantly reduced TNFα secretion in a dose-dependent fashion. In contrast, no such reductions were observed in cells treated with control anti-mIgG antibody. These findings demonstrated a partial reduction in TNFα expression following inhibition of the CD14 receptor pathway that was similar in magnitude to the effects observed when Rac1 was inhibited by N17Rac1 expression. To begin to address whether Rac1 acts through CD14-dependent or -independent pathways, the level of GTP bound, activated Rac1 was assessed following treatment of RAW cells with anti-CD14 antibodies in the presence or absence of N17Rac1 expression. If Rac1 activation occurred through a pathway independent of CD14, we would expect to see no effect of anti-CD14 on the level of GTP bound Rac1. Results from this analysis (Fig. 9*B*) are consistent with the hypothesis that Rac1 is independent of CD14, since the blocking antibodies had no detectable influence on Rac1 activation. In contrast, N17Rac1 expression clearly decreased the level of GTP bound Rac1. We hypothesized that if these two pathways are acting in parallel, treatment with CD14 blocking antibodies and Ad.N17Rac1 should be capable of inhibiting the majority of TNFα production following LPS stimulation. As anticipated, combined inhibition of Rac1 and CD14-dependent pathways demonstrated an additive effect on reducing TNFα secretion (74 ± 6%), which was greater than inhibiting Rac1 (44 ± 6%) or CD14 (35 ± 7%) individually (Fig. 9*C*). These effects demonstrated a clear dose response to inhibitor (*i.e.* multiplicity of infection of Ad.N17Rac1 or concentration of anti-CD14 antibody) and were not seen with the control vector Ad.CMVLacZ or with the control isotype matched antibody. In summary, our overall findings suggest that LPS-induced Rac1 activation stimulates NFκB activation and subsequent TNFα expression through ROS production in a CD14-independent manner.

LPS Differentially Regulates the Expression of TLR in RAW Cells—Results thus far have suggested that Rac1 mediates LPS activation of NFκB through the production of ROS by a mechanism that is independent of CD14. However, the identity of the Rac1-linked receptor remains unknown. LPS is known to exert its effects on cells through the activation of Toll-like receptors. To date, numerous murine *TLR* genes have been identified (65). TLR4 is widely accepted as a primary mammalian LPS sensor (66, 67).

Although the function of TLR2 is somewhat controversial (68, 69), TLR2 has also been shown to mediate LPS-induced cellular signaling (70, 71). Interestingly, it has been recently reported that *Staphylococcus aureus* induction of *TLR2* leads to Rac1-dependent NFκB activation in THP-1 cells (72). Importantly, oligomerization of TLR receptors has been suggested to create LPS-specific signaling receptors functionally distinct from the conventional CD14-TLR4 pathway (73). For example, TLR6 and TLR2 have been shown to cooperate in the activation

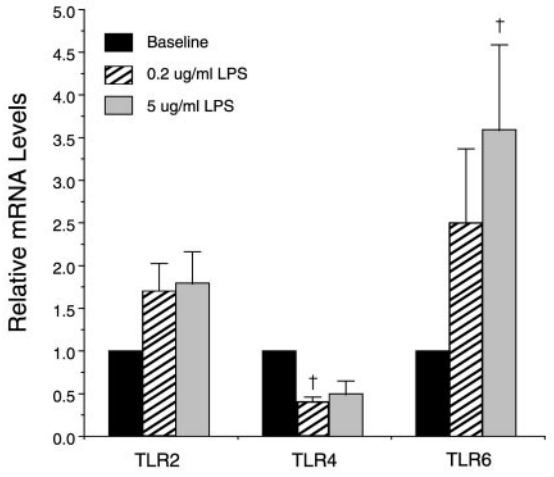

FIG. 10. **LPS differentially regulates the expression of *TLR* genes.** Relative mRNA expression levels of various *TLR* genes (*TLR2, TLR4*, and *TLR6*) were determined in LPS-treated or untreated controls using real time-PCR as described under "Experimental Procedures." RAW cells were treated with 0.2 and 5 μg/ml LPS for 4 h at 37 °C prior to analysis. For each sample, *TLR* mRNA levels were normalized to *HPRT* as an internal control. For each *TLR* gene, untreated controls were chosen as the reference point to which all LPS-treated experimental samples were compared (untreated controls are normalized to 1). Data represent the mean (±S.E.) of four independent experiments. A statistically significant difference between untreated and LPS-treated samples, as determined by the paired Student's *t* test ($p < 0.05$), is denoted by †.

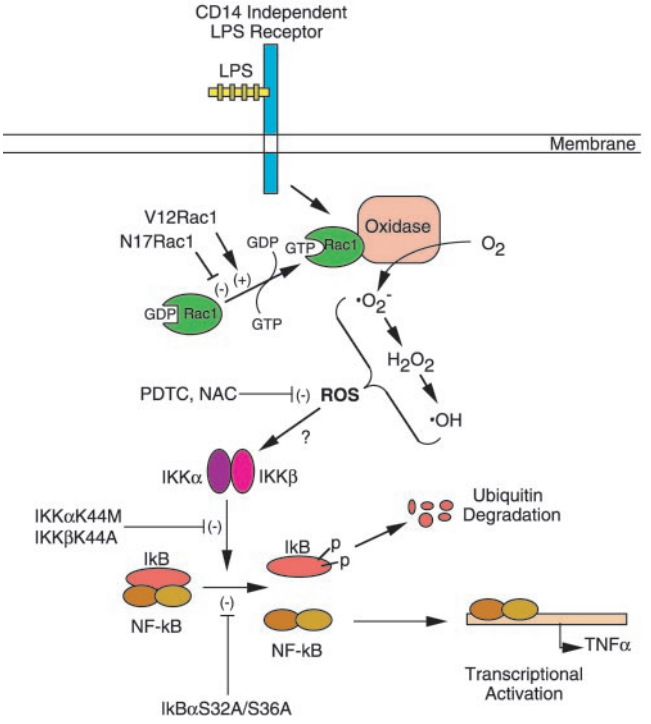

FIG. 11. **Schematic model for the role of Rac1 in LPS-mediated NFκB activation.** Our results suggest the existence of an alternative ROS-dependent Rac1 activation pathway, which appears to be independent of the CD14 receptor but still capable of activating NFκB-mediated TNFα expression. As shown, a dominant inactive form of Rac1 (N17Rac1) or ROS scavengers (PDTC and NAC) inhibit the production of ROS, NFκB activation, and TNFα production. In contrast, a constitutively active form of Rac1 (V12Rac1) augments these events. Both IKKα and IKKβ appear to be involved in Rac1-mediated NFκB activation. This is supported by the finding that the dominant mutants IKKα(K44M), IKKβ(K44A), and IkBα(S32A/S36A) all inhibit NFκB activation following expression of V12Rac1. The LPS receptor that interacts with Rac1 in this pathway is currently unknown.

of NFκB leading to TNFα expression in RAW cells (74). For these reasons, we examined the expression levels of *TLR2, TLR4*, and *TLR6* following LPS stimulation of RAW cells using real time PCR. We reasoned that such information would prove valuable for the identification of candidate receptors responsible for ROS formation following LPS stimulation. To this end, RAW cells were treated with LPS at concentrations of 0.2 or 5 μg/ml for 4 h and potential alterations in *TLR* mRNA levels were analyzed (Fig. 10). Our results indicated that the relative level of *TLR4* mRNA was reduced by 60% following LPS exposure as compared with a 70% increase in *TLR2* mRNA. Interestingly, a 3-fold induction in *TLR6* mRNA levels was detected after 4 h of LPS treatment. Our findings demonstrating an increase in *TLR2* mRNA levels and a decrease in *TLR4* mRNA levels following LPS challenge substantiate previously published recent reports (75–77). The unique aspect of our finding, which has not been previously reported, is the up-regulation of *TLR6* mRNA following LPS exposure. These results suggest that TLR2, TLR4, and TLR6 are all potential candidates that could mediate Rac1 activation in RAW cells. Furthermore, mRNA levels of these genes are differentially modulated following LPS challenge. The significance of these changes in response to LPS and the potential involvement of these Toll-like receptors in Rac1 signaling remain to be determined.

DISCUSSION

The number of deaths due to sepsis continues to rise worldwide (3). Despite extensive research, efficacious therapies for sepsis have yet to be developed (78). Moreover, clinical trials using either pharmacological agents or monoclonal anti-endotoxin antibodies have not been successful (79–82). The failure to develop effective therapies for septic shock is partly due to our limited understanding of the signaling pathways involved in the generation of the septic proinflammatory state.

In the present report, we have provided the first description of a pathway linking the small GTP-binding protein Rac1 to LPS-stimulated ROS generation, NFκB transcriptional activation, and subsequent TNFα expression (Fig. 11). Several key features of LPS-induced Rac1 signal transduction should be noted. First, inhibition of Rac1 with the dominant negative mutant N17Rac1 blocked about half of both NFκB transcriptional activation and the LPS-induced TNFα response. The same negative mutant blocked the majority of ROS formation induced by LPS. Second, the expression of the constitutively active form of Rac1 was capable of mimicking LPS-induced ROS formation, NFκB activation, and TNFα induction in the absence of endotoxin stimulation. Third, chemical antioxidants blocked the majority of the LPS-induced NFκB transcriptional activation and only a fraction (~50%) of TNFα expression. Fourth, we have clearly shown that LPS treatment leads to the generation of superoxide radicals. Together, these findings suggest that LPS-induced Rac1 activation acts primarily to induce TNFα through a ROS-dependent NFκB pathway.

Although the link between LPS activation of Rac1 and subsequent induction of NFκB is strong, other pathways independent of Rac1 are also likely to influence the total level of NFκB activation and TNFα production following LPS treatment. This is indicated by the finding that N17Rac1 expression blocked only half of the LPS-induced NFκB DNA binding and transcriptional activity. If the inhibition of Rac1 by the dominant negative mutant were indeed complete (as was suggested by activity assays for GTP bound Rac1), this would suggest that other LPS-induced pathways must also activate NFκB. In contrast, V12Rac1 induction of NFκB and TNFα expression was nearly completely blocked by expression of the IκBα dominant mutant, suggesting that although multiple LPS-stimulated pathways may activate NFκB, the Rac1 component appears to in-

duce TNFα primarily through NFκB activation. Parallel pathways involved in NFκB activation, which converge at the level of the IKK complex, have previously been identified (83). These studies have demonstrated that NIK and MEKK1 can independently activate the IKK complex through distinct regulation of IKKα and IKKβ. In the case of LPS stimulation, our studies demonstrate that both IKKα and IKKβ play a role in the activation of TNFα expression. Similar effects of these IKK mutants on TNFα expression were noted in V12Rac1 expressing cells, supporting the notion that the IKK complex is a predominant target of LPS-mediated Rac1 activation. Interestingly, the inhibition of IKKβ more significantly attenuated (18–30-fold) NFκB activation than did inhibition of IKKα, as noted in luciferase assays of LPS-treated and V12Rac1-expressing cells. Such findings suggest that IKKβ plays a more dominant role than IKKα as an effector of Rac1 activation of NFκB.

Our studies using CD14 blocking antibodies suggest that LPS-mediated Rac1 activation of NFκB and TNFα may be independent of the CD14 receptor. Testing LPS-induced Rac1 activation in CD14-deficient murine macrophages may confirm these observations. In this regard, CD14-dependent pathways of sepsis have recently been identified and they are increasing in number (66, 84–86). Human macrophage receptors other than CD14, such as CD11/CD18 integrins, have also been reported to bind to the lipid A region of Gram-negative bacteria (87, 88). Similar levels of TNFα release were observed from CD14-deficient and wild type macrophages stimulated by whole *E. coli* (89). In this particular case, it was demonstrated that CD11b/CD18 receptors compensated for LPS responsiveness in the absence of CD14 receptor. The fact that intracellular Toll-like receptor activation can initiate signaling pathways, in the absence of CD14 and long after particle internalization in phagolysosomes, should also be considered (90). It is also interesting to note that lipopolysaccharide structure can influence the pathways activated in LPS-induced macrophage response (*i.e.* CD14-dependent *versus* CD14-independent (25)).

It is believed that CD11b/CD18 integrin-mediated LPS responsiveness is conducted through the same downstream signaling elements as CD14 (91–94). Therefore, although Rac1 responsiveness appears to be CD14 independent in our preliminary studies, this would not rule out the possibility that similar downstream molecules (MYD88, IRAK, and TRAF6 etc.) are involved in LPS-induced Rac1 signaling. It should be noted, however, in our studies the effects of inhibiting both CD14 and Rac1 were additive, indicating the possibility of differences in the pathways. Consequently, from a therapeutic standpoint, our studies suggest that dual inhibition of both CD14 and Rac1-dependent pathways may provide the most efficacious strategies for inhibiting proinflammatory cytokine production induced by LPS in the course of sepsis.

Acknowledgments—We gratefully acknowledge Sean Martin and Garry Buettner at the ESR Facility of the University of Iowa for help with ESR analysis.

REFERENCES

1. Pinner, R. W., Teutsch, S. M., Simonsen, L., Klug, L. A., Graber, J. M., Clarke, M. J., and Berkelman, R. L. (1996) *J. Am. Med. Assoc.* **275,** 189–193
2. Bone, R. C. (1991) *Chest* **100,** 802–808
3. Bone, R. C., Grodzin, C. J., and Balk, R. A. (1997) *Chest* **112,** 235–243
4. Doe, W. F., Yang, S. T., Morrison, D. C., Betz, S. J., and Henson, P. M. (1978) *J. Exp. Med.* **148,** 557–568
5. Ulevitch, R. J., and Tobias, P. S. (1995) *Annu. Rev. Immunol.* **13,** 437–457
6. Schletter, J., Heine, H., Ulmer, A. J., and Rietschel, E. T. (1995) *Arch. Microbiol.* **164,** 383–389
7. Medvedev, A. E., Kopydlowski, K. M., and Vogel, S. N. (2000) *J. Immunol.* **164,** 5564–5574
8. Morrison, D. C., and Ulevitch, R. J. (1978) *Am. J. Pathol.* **93,** 526–617
9. Raetz, C. R., Ulevitch, R. J., Wright, S. D., Sibley, C. H., Ding, A., and Nathan, C. F. (1991) *FASEB J.* **5,** 2652–2660
10. Dentener, M. A., Von Asmuth, E. J., Francot, G. J., Marra, M. N., and Buurman, W. A. (1993) *J. Immunol.* **151,** 4258–4265
11. Wright, S. D., Ramos, R. A., Tobias, P. S., Ulevitch, R. J., and Mathison, J. C. (1990) *Science* **249,** 1431–1433
12. Wright, S. D., Ramos, R. A., Hermanowski-Vosatka, A., Rockwell, P., and Detmers, P. A. (1991) *J. Exp. Med.* **173,** 1281–1286
13. Schletter, J., Brade, H., Brade, L., Kruger, C., Loppnow, H., Kusumoto, S., Rietschel, E. T., Flad, H. D., and Ulmer, A. J. (1995) *Infect. Immun.* **63,** 2576–2580
14. Dentener, M. A., Bazil, V., Von Asmuth, E. J., Ceska, M., and Buurman, W. A. (1993) *J. Immunol.* **150,** 2885–2891
15. Fearns, C., Kravchenko, V. V., Ulevitch, R. J., and Loskutoff, D. J. (1995) *J. Exp. Med.* **181,** 857–866
16. Ziegler-Heitbrock, H. W., and Ulevitch, R. J. (1993) *Immunol. Today* **14,** 121–125
17. Ulevitch, R. J. (1993) *Adv. Immunol.* **53,** 267–289
18. Heumann, D., Gallay, P., Barras, C., Zaech, P., Ulevitch, R. J., Tobias, P. S., Glauser, M. P., and Baumgartner, J. D. (1992) *J. Immunol.* **148,** 3505–3512
19. Corradin, S. B., Mauel, J., Gallay, P., Heumann, D., Ulevitch, R. J., and Tobias, P. S. (1992) *J. Leukocyte Biol.* **52,** 363–368
20. Schumann, R. R., Leong, S. R., Flaggs, G. W., Gray, P. W., Wright, S. D., Mathison, J. C., Tobias, P. S., and Ulevitch, R. J. (1990) *Science* **249,** 1429–1431
21. Meszaros, K., Aberle, S., Dedrick, R., Machovich, R., Horwitz, A., Birr, C., Theofan, G., and Parent, J. B. (1994) *Blood* **83,** 2516–2525
22. Theofan, G., Horwitz, A. H., Williams, R. E., Liu, P. S., Chan, I., Birr, C., Carroll, S. F., Meszaros, K., Parent, J. B., Kasler, H., Aberle, S., Trown, P. W., and Gazzano-Santoro, H. (1994) *J. Immunol.* **152,** 3623–3629
23. Schuster, J. M., and Nelson, P. S. (2000) *J. Leukocyte Biol.* **67,** 767–773
24. Netea, M. G., Kullberg, B. J., and van der Meer, J. W. (1998) *Immunology* **94,** 340–344
25. Gangloff, S. C., Hijiya, N., Haziot, A., and Goyert, S. M. (1999) *Clin. Infect. Dis.* **28,** 491–496
26. Peppelenbosch, M. P., DeSmedt, M., ten Hove, T., van Deventer, S. J., and Grooten, J. (1999) *Blood* **93,** 4011–4018
27. Kimura, S., Tamamura, T., Nakagawa, I., Koga, T., Fujiwara, T., and Hamada, S. (2000) *Scand. J. Immunol.* **51,** 392–399
28. Lynn, W. A., Liu, Y., and Golenbock, D. T. (1993) *Infect. Immun.* **61,** 4452–4461
29. Jungi, T. W., Sager, H., Adler, H., Brcic, M., and Pfister, H. (1997) *Infect. Immun.* **65,** 3577–3584
30. Boxer, G. J., Curnutte, J. T., and Boxer, L. A. (1985) *Hosp. Pract.* **20,** 69–73; 77; 80
31. DeLeo, F. R., Renee, J., McCormick, S., Nakamura, M., Apicella, M., Weiss, J. P., and Nauseef, W. M. (1998) *J. Clin. Invest.* **101,** 455–463
32. Joneson, T., and Bar-Sagi, D. (1998) *J. Biol. Chem.* **273,** 17991–17994
33. Olson, M. F., Ashworth, A., and Hall, A. (1995) *Science* **269,** 1270–1272
34. Fisher, K. J., Gao, G. P., Weitzman, M. D., DeMatteo, R., Burda, J. F., and Wilson, J. M. (1996) *J. Virol.* **70,** 520–532
35. Brown, M. R., Miller, F. J., Jr., Li, W. G., Ellingson, A. N., Mozena, J. D., Chatterjee, P., Engelhardt, J. F., Zwacka, R. M., Oberley, L. W., Fang, X., Spector, A. A., and Weintraub, N. L. (1999) *Circ. Res.* **85,** 524–533
36. Kim, K. S., Takeda, K., Sethi, R., Pracyk, J. B., Tanaka, K., Zhou, Y. F., Yu, Z. X., Ferrans, V. J., Bruder, J. T., Kovesdi, I., Irani, K., Goldschmidt-Clermont, P., and Finkel, T. (1998) *J. Clin. Invest.* **101,** 1821–1826
37. Sulciner, D. J., Irani, K., Yu, Z. X., Ferrans, V. J., Goldschmidt-Clermont, P., and Finkel, T. (1996) *Mol. Cell. Biol.* **16,** 7115–7121
38. Iimuro, Y., Nishiura, T., Hellerbrand, C., Behrns, K. E., Schoonhoven, R., Grisham, J. W., and Brenner, D. A. (1998) *J. Clin. Invest.* **101,** 802–811
39. Zandi, E., Rothwarf, D. M., Delhase, M., Hayakawa, M., and Karin, M. (1997) *Cell* **91,** 243–252
40. Anderson, R. D., Haskell, R. E., Xia, H., Roessler, B. J., and Davidson, B. L. (2000) *Gene Ther.* **7,** 1034–1038
41. Engelhardt, J. F., Yang, Y., Stratford-Perricaudet, L. D., Allen, E. D., Kozarsky, K., Perricaudet, M., Yankaskas, J. R., and Wilson, J. M. (1993) *Nat. Genet.* **4,** 27–34
42. Glaven, J. A., Whitehead, I., Bagrodia, S., Kay, R., and Cerione, R. A. (1999) *J. Biol. Chem.* **274,** 2279–2285
43. Bagrodia, S., Taylor, S. J., Jordon, K. A., Van Aelst, L., and Cerione, R. A. (1998) *J. Biol. Chem.* **273,** 23633–23636
44. Andrews, N. C., and Faller, D. V. (1991) *Nucleic Acids Res.* **19,** 2499
45. Sanlioglu-Crisman, S., and Oberdick, J. (1997) *Prog. Brain Res.* **114,** 3–19
46. Sanlioglu, S., and Engelhardt, J. (1999) *Gene Ther.* **6,** 1427–1437
47. Miller, F. J., Jr., Gutterman, D. D., Rios, C. D., Heistad, D. D., and Davidson, B. L. (1998) *Circ. Res.* **82,** 1298–1305
48. Chandel, N. S., Trzyna, W. C., McClintock, D. S., and Schumacker, P. T. (2000) *J. Immunol.* **165,** 1013–1021
49. Peristeris, P., Clark, B. D., Gatti, S., Faggioni, R., Mantovani, A., Mengozzi, M., Orencole, S. F., Sironi, M., and Ghezzi, P. (1992) *Cell. Immunol.* **140,** 390–399
50. Wahl, C., Liptay, S., Adler, G., and Schmid, R. M. (1998) *J. Clin. Invest.* **101,** 1163–1174
51. Delhase, M., Hayakawa, M., Chen, Y., and Karin, M. (1999) *Science* **284,** 309–313
52. Hu, Y., Baud, V., Delhase, M., Zhang, P., Deerinck, T., Ellisman, M., Johnson, R., and Karin, M. (1999) *Science* **284,** 316–320
53. De Deken, X., Wang, D., Many, M. C., Costagliola, S., Libert, F., Vassart, G., Dumont, J. E., and Miot, F. (2000) *J. Biol. Chem.* **275,** 23227–23233
54. Suh, Y. A., Arnold, R. S., Lassegue, B., Shi, J., Xu, X., Sorescu, D., Chung, A. B., Griendling, K. K., and Lambeth, J. D. (1999) *Nature* **401,** 79–82
55. Gorlach, A., Brandes, R. P., Nguyen, K., Amidi, M., Dehghani, F., and Busse, R. (2000) *Circ. Res.* **87,** 26–32

56. Finkelstein, E., Rosen, G. M., and Rauckman, E. J. (1980) *Arch. Biochem. Biophys* **200,** 1–16
57. Zweier, J. L., Kuppusamy, P., and Lutty, G. A. (1988) *Proc. Natl. Acad. Sci. U. S. A.* **85,** 4046–4050
58. Zweier, J. L., Kuppusamy, P., Thompson-Gorman, S., Klunk, D., and Lutty, G. A. (1994) *Am. J. Physiol.* **266,** C700–708
59. Carter, W. O., Narayanan, P. K., and Robinson, J. P. (1994) *J. Leukocyte Biol.* **55,** 253–258
60. Shi, X., Leonard, S. S., Wang, S., and Ding, M. (2000) *Ann. Clin. Lab. Sci.* **30,** 209–216
61. Gillissen, A., Scharling, B., Jaworska, M., Bartling, A., Rasche, K., and Schultze-Werninghaus, G. (1997) *Res. Exp. Med.* **196,** 389–398
62. Aruoma, O. I., Halliwell, B., Hoey, B. M., and Butler, J. (1989) *Free Radic. Biol. Med.* **6,** 593–597
63. Miyata, Y., Takeda, H., Kitano, S., and Hanazawa, S. (1997) *Infect. Immun.* **65,** 3513–3519
64. Hattor, Y., Kasai, K., Akimoto, K., and Thiemermann, C. (1997) *Biochem. Biophys. Res. Commun.* **233,** 375–379
65. Rock, F. L., Hardiman, G., Timans, J. C., Kastelein, R. A., and Bazan, J. F. (1998) *Proc. Natl. Acad. Sci. U. S. A.* **95,** 588–593
66. Lien, E., Means, T. K., Heine, H., Yoshimura, A., Kusumoto, S., Fukase, K., Fenton, M. J., Oikawa, M., Qureshi, N., Monks, B., Finberg, R. W., Ingalls, R. R., and Golenbock, D. T. (2000) *J. Clin. Invest.* **105,** 497–504
67. Beutler, B. (2000) *Curr. Opin. Immunol.* **12,** 20–26
68. Tapping, R. I., Akashi, S., Miyake, K., Godowski, P. J., and Tobias, P. S. (2000) *J. Immunol.* **165,** 5780–5787
69. Hirschfeld, M., Ma, Y., Weis, J. H., Vogel, S. N., and Weis, J. J. (2000) *J. Immunol.* **165,** 618–622
70. Yang, R. B., Mark, M. R., Gray, A., Huang, A., Xie, M. H., Zhang, M., Goddard, A., Wood, W. I., Gurney, A. L., and Godowski, P. J. (1998) *Nature* **395,** 284–288
71. Werts, C., Tapping, R. I., Mathison, J. C., Chuang, T. H., Kravchenko, V., Saint Girons, I., Haake, D. A., Godowski, P. J., Hayashi, F., Ozinsky, A., Underhill, D. M., Kirschning, C. J., Wagner, H., Aderem, A., Tobias, P. S., and Ulevitch, R. J. (2001) *Nat. Immunol.* **2,** 346–352
72. Arbibe, L., Mira, J. P., Teusch, N., Kline, L., Guha, M., Mackman, N., Godowski, P. J., Ulevitch, R. J., and Knaus, U. G. (2000) *Nat. Immunol.* **1,** 533–540
73. Perera, P. Y., Mayadas, T. N., Takeuchi, O., Akira, S., Zaks-Zilberman, M., Goyert, S. M., and Vogel, S. N. (2001) *J. Immunol.* **166,** 574–581
74. Ozinsky, A., Underhill, D. M., Fontenot, J. D., Hajjar, A. M., Smith, K. D., Wilson, C. B., Schroeder, L., and Aderem, A. (2000) *Proc. Natl. Acad. Sci. U. S. A.* **97,** 13766–13771
75. Liu, Y., Wang, Y., Yamakuchi, M., Isowaki, S., Nagata, E., Kanmura, Y., Kitajima, I., and Maruyama, I. (2001) *Infect. Immun.* **69,** 2788–2796
76. Matsuguchi, T., Musikacharoen, T., Ogawa, T., and Yoshikai, Y. (2000) *J. Immunol.* **165,** 5767–5772
77. Nomura, F., Akashi, S., Sakao, Y., Sato, S., Kawai, T., Matsumoto, M., Nakanishi, K., Kimoto, M., Miyake, K., Takeda, K., and Akira, S. (2000) *J. Immunol.* **164,** 3476–3479
78. Bone, R. C. (1996) *J. Am. Med. Assoc.* **276,** 565–566
79. Ziegler, E. J., Fisher, C. J., Jr., Sprung, C. L., Straube, R. C., Sadoff, J. C., Foulke, G. E., Wortel, C. H., Fink, M. P., Dellinger, R. P., Teng, N. N., Allen, E. I., Berger, H. J., Knatterud, G. L., LoBuglio, A. F., Smith, C. R., and the HA-1A Sepsis Study Group (1991) *N. Engl. J. Med.* **324,** 429–36
80. McCloskey, R. V., Straube, R. C., Sanders, C., Smith, S. M., and Smith, C. R. (1994) *Ann. Intern. Med.* **121,** 1–5
81. Bone, R. C., Balk, R. A., Fein, A. M., Perl, T. M., Wenzel, R. P., Reines, H. D., Quenzer, R. W., Iberti, T. J., Macintyre, N., and Schein, R. M. (1995) *Crit. Care Med.* **23,** 994–1006
82. Bone, R. C. (1995) *Chest* **107,** 298–299
83. Nakano, H., Shindo, M., Sakon, S., Nishinaka, S., Mihara, M., Yagita, H., and Okumura, K. (1998) *Proc. Natl. Acad. Sci. U. S. A.* **95,** 3537–3542
84. Kirschning, C. J., Wesche, H., Merrill Ayres, T., and Rothe, M. (1998) *J. Exp. Med.* **188,** 2091–2097
85. Medzhitov, R., Preston-Hurlburt, P., Kopp, E., Stadlen, A., Chen, C., Ghosh, S., and Janeway, C. A., Jr. (1998) *Mol. Cell.* **2,** 253–258
86. Hoffmann, J. A., Kafatos, F. C., Janeway, C. A., and Ezekowitz, R. A. (1999) *Science* **284,** 1313–1318
87. Wright, S. D., and Jong, M. T. (1986) *J. Exp. Med.* **164,** 1876–1888
88. Wright, S. D., Levin, S. M., Jong, M. T., Chad, Z., and Kabbash, L. G. (1989) *J. Exp. Med.* **169,** 175–183
89. Moore, K. J., Andersson, L. P., Ingalls, R. R., Monks, B. G., Li, R., Arnaout, M. A., Golenbock, D. T., and Freeman, M. W. (2000) *J. Immunol.* **165,** 4272–4280
90. Underhill, D. M., Ozinsky, A., Hajjar, A. M., Stevens, A., Wilson, C. B., Bassetti, M., and Aderem, A. (1999) *Nature* **401,** 811–815
91. Ingalls, R. R., and Golenbock, D. T. (1995) *J. Exp. Med.* **181,** 1473–1479
92. Flaherty, S. F., Golenbock, D. T., Milham, F. H., and Ingalls, R. R. (1997) *J. Surg. Res.* **73,** 85–89
93. Ingalls, R. R., Arnaout, M. A., Delude, R. L., Flaherty, S., Savedra, R., Jr., and Golenbock, D. T. (1998) *Prog. Clin. Biol. Res.* **397,** 107–117
94. Ingalls, R. R., Arnaout, M. A., and Golenbock, D. T. (1997) *J. Immunol.* **159,** 433–438